Photoinduced Localization of Orientationally Ordered Polymer Networks at the Surface of a Liquid Crystal Host

S. W. Kang,[†] S. Sprunt,[‡] and L. C. Chien*[,†]

Chemical Physics Interdisciplinary Program and Liquid Crystal Institute, and Department of Physics, Kent State University, Kent, Ohio 44242

Received April 11, 2002; Revised Manuscript Received August 2, 2002

ABSTRACT: We demonstrated liquid crystalline template-directed and photoinduced localization of orientationally ordered polymer networks in a liquid crystal host. In the limit of a diffusion-controlled polymerization process, the location of these networks in a liquid crystal (LC) cell can be controlled by varying the wavelength-dependent absorption coefficient of the UV radiation used to initiate photopolymerization. Specific results are presented for a bulk polymer network (obtained when $\lambda = 365$ nm) and a micrometer-thick polymer surface layer (for $\lambda = 322$ nm), both of which are produced in similar LC cells, using the same 5 wt % initial concentration of a liquid crystalline diacrylate, and for both planar and homeotropic orientations of the liquid crystal director. The surface-localized networks have minimal impact on the desirable electrooptic properties of the host, such as low operating voltage and minimal scattering loss. We discuss predictive models for surface localization in the opposite limits of "infinite" and zero monomer diffusion constant.

Introduction

In recent years, polymer−liquid crystal composites have provided fertile ground for the development of various electrooptical devices, including high performance flat panel displays,[1−5] electrically switchable diffraction gratings,[6−10] and electrically tunable microlens assemblies.[11] These composites may be classified into "droplet" systems, in which liquid crystal droplets are dispersed in a relatively high concentration of polymer, and "network" systems, in which a low concentration polymer network stabilizes various bulk states of the liquid crystal host. When aligned nematic or cholesteric hosts are used with liquid crystalline monomers, the polymer network efficiently captures the local orientational order.[2,12−16]

The templating effect is more dramatic when the networks are formed in various pattern-forming states of liquid crystals.[14−16] In this case, one may produce three-dimensional networks with variable degrees of orientational *and* positional order (achieved through highly patterned phase separation). The diversity of these structures, and the possibilities for rationally manipulating that diversity, make the "network" systems very attractive for tuning electrooptical device parameters such as switching voltage and time, diffraction efficiency, and light loss, which are largely determined by the morphological details of the polymer−liquid crystal interface. Liquid-crystal-based templating becomes even more intriguing when one considers the possibilities of patterning functionalized networks (e.g., networks of photonic or electronic materials) through what is fundamentally a self-assembly process.

Choice of materials, the initial state of orientational order of the liquid crystal, and the use of photopolymerization are all known to be useful means to control bulk network morphology.[17−20] Spatial variations in host orientational order or in light intensity have proven to be flexible tools for *bulk* patterning of polymer networks.[6−8,14−16,21] For example, in pioneering work, Broer et al.[22] and Hikmet et al.[23] used a planar-aligned cholesteric phase, a chiral monomer, and photoinduced monomer diffusion to produce and then lock in a gradient in pitch through the bulk sample, resulting in a broadband reflector. Comparatively little is known, however, about the potential for strongly localizing ordered networks in a thin layer at the interface between a substrate and the liquid crystal host. This case is quite interesting, because the network structure may then have a desired stabilizing effect on the bulk state of the LC orientational order, without compromising its electrooptic performance (e.g., maintaining a low threshold voltage for electrooptic switching) or providing unwanted optical contrast with the LC throughout the cell interior (leading, e.g., to high scattering losses).

It is the purpose of this paper to demonstrate the potential for control over the network distribution in the "third" dimension—between the surfaces of the host LC and perpendicular to the UV wave front—by the relatively simple means of selecting the wavelength of UV light used in photopolymerization to be inside or outside a carefully characterized absorption band. In this way, we demonstrate that a crossover from bulk to surface-localized networks is achievable by a simple modification of the photoinduced monomer diffusion process. For the two conventional types of LC orientation on flat substrates (homogeneous/planar and homeotropic/vertical orientation), we clearly demonstrate templating of the polymer network by the LC at an interface. Moreover, when an intially planar-aligned LC is reoriented by applied field into the homeotropic state, and a surface network is then templated on this state, the bulk LC remains homeotropically aligned when the field is removed. Thus, a templated network at the interface can completely reverse the effect of even strong initial anchoring conditions due to the particular substrate. We further show that while a bulk network strongly modi-

* To whom correspondence should be addressed: lcchien@lci.kent.edu.
[†] Chemical Physics Interdisciplinary Program and Liquid Crystal Institute, Kent State University.
[‡] Department of Physics, Kent State University.

10.1021/ma020578o CCC: $22.00
Published on Web 10/30/2002

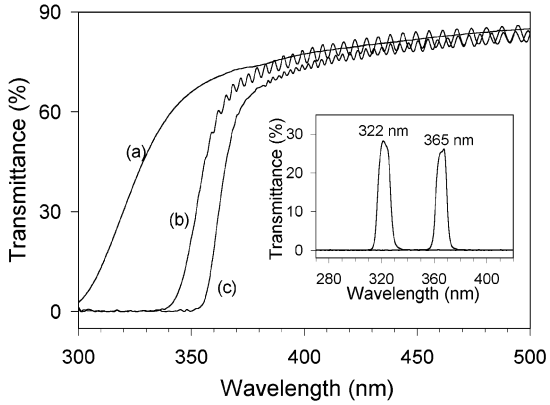

Figure 1. (a) Optical transmittance of a single substrate (including alignment and electrode layers). (b) Transmittance of a sample cell filled with homogeneously aligned nematic mixture BL006, 5 wt % RM257, and 0.2 wt % photoinitiator prior to photopolymerization. The incident light is polarized perpendicular to the optic axis. (c) Same as part b, except the incident polarization is parallel to the optic axis. Inset: Transmittance of the band-pass filters used in our experiments.

fies the threshold field for director reorientation, the surface network has essentially no effect on the bulk elastic properties—i.e., it behaves as a conventional alignment layer in this respect.

Experimental Section

Sample Preparation. Samples were prepared by mixing nematic LC BL006 (94.8 wt %, a eutectic mixture of several low-molar-mass LCs from Merck), reactive nematic monomer RM257 (5 wt %, 1,4-bis[3-(acryloyloxy)propyloxy]-2-methylbenzene, crystal to nematic 70 °C and nematic to isotropic 126 °C, Merck), and photoinitiator Irgacure 651 (0.2%, 2,2-dimethoxy-2-phenly acetophenone, Ciba Additive). After the mixture of liquid crystal, monomer, and photoinitiator was heated to the isotropic temperature of the liquid crystal for a short time, the mixture was cooled to room temperature and filled into LC cells by a capillary action. Commercially available LC cells (EHC, Japan), assembled with indium−tin−oxide coated conductive glass substrates and separated with 10-μm glass sphere spacers, were used in this study. For homogeneous LC alignment with a small pretilt angle, the inner surfaces of the substrates were coated with polyimide alignment layers, which were uniaxially rubbed and assembled at a 180° angle with respect to each rubbing direction, over transparent electrodes.

Photopolymerization. A different wavelength of UV light was selected for photopolymerization in each LC alignment. Polymer networks were formed by photopolymerization using collimated, unpolarized UV light from a 150 W xenon lamp (Oriel 6258), which was applied for 30 min at normal incidence to the sample. Two wavelengths, 322 and 365 nm (selected by band-pass filters), were used at incident intensities of 0.08 and 0.04 mW/cm^2 intensity, respectively. The higher intensity for 322 nm compensated for a factor of 2 higher absorption by the substrates measured at this wavelength (see Figure 1a).

Optical Texture and Polymer Network Morphology. Polarizing optical microscopy was performed with a Nikon OPTIPHOT2-POL, with the polarizer and analyzer crossed. The samples were prepared by preferentially dissolving the liquid crystal using a 70/30 v/v mixture of hexane and dichloromethane, with the solvent refreshed seven times over 7 days. The cells were carefully opened to minimize any disturbance of the structure of the polymer networks, and a thin gold layer was deposited. The polymer network morphology was then observed using a JEOL JSM-6300V scanning electron microscope operated at 10 kV in secondary electron imaging mode. The morphology was completely consistent over many individual samples subjected to the same procedure, and no evidence of damage to the network was detected.

Capacitance Measurement. The response of the liquid crystal host to applied voltages for surface and bulk polymer network morphologies was evaluated by monitoring the cell capacitance using both a commercial LCR meter (HP 4284A) and a lock-in amplifier (Stanford Research, model SR-830). The latter measured real and imaginary parts of the current through the cell due to a 10 kHz sinusoidal applied voltage.

Results and Discussion

In our experiments, photopolymerization was carried out at room temperature using a fixed UV light intensity (and accounting for the wavelength dependence of the incident substrate absorption). The UV absorption spectrum of our samples was carefully characterized in order to determine appropriate wavelengths for surface localization of the polymer network (high absorption limit) and bulk network development (low absorption limit). Figure 1, curve a, shows the UV−vis absorption for a single substrate illuminated with unpolarized light. Since nematic liquid crystals are dichroic, absorption spectra for filled cells were measured for polarizations perpendicular (Figure 1, curve b) and parallel (Figure 1, curve c) to a uniform, homogeneously aligned director. Using a band-pass filter centered on 322 nm (see inset) and comparing curve a to curves b and c, we see that the incident UV power is strongly absorbed by the liquid crystal mixture for both polarizations in the bulk of our 10-μm thick sample. Thus, the 322 nm wavelength produces a strong gradient in UV intensity across the sample thickness, and is a prospective choice for surface localization. In contrast, transmission of a narrow band of unpolarized light centered on 365 nm is limited mainly by substrate absorption, and therefore is an appropriate choice for formation of a bulk network.

Morphologies for surface and bulk RM257 networks formed in homogeneously and homeotropically aligned nematic hosts are shown in Figures 2 and 3, respectively. The SEM images were taken at a 45° angle to the substrate normal. The bottom part of each image shows a horizontal section of the bare substrate, which was masked from UV exposure during photopolymerization. (The UV light is normally incident from below in all cases shown.) Figure 2a displays the bulk network formed under 365 nm exposure; correcting for the tilted view, the network has a uniform structure and density across the full 10 μm sample thickness. The top surface of the image reveals well-formed polymer fibrils running horizontally and parallel to the host alignment direction. The featureless, "smooth" profile of the network at the edge of the exposed region (about midway in the figure) is an artifact of the photomask; the true internal structure is fibrillike. Approximately equivalent domains to that shown were observed on both UV incident and far-side substrates in random areas of the cell. After similar exposure conditions applied for 322 nm UV light, a similar, fibril morphology was recorded (Figure 2b), but the network was entirely localized into a thin layer on the substrate nearest to UV light. The inset to Figure 2b, obtained after scribing the sample to obtain a sharp depth profile, reveals a layer thickness under or close to 1 μm. There is negligible polymer network formed on the opposite surface.

Figure 3 shows SEM results for the case of homeotropic liquid crystal orientation, which was obtained starting with the same initial conditions as in Figure 2 (LC molecules/director in the substrate plane) and

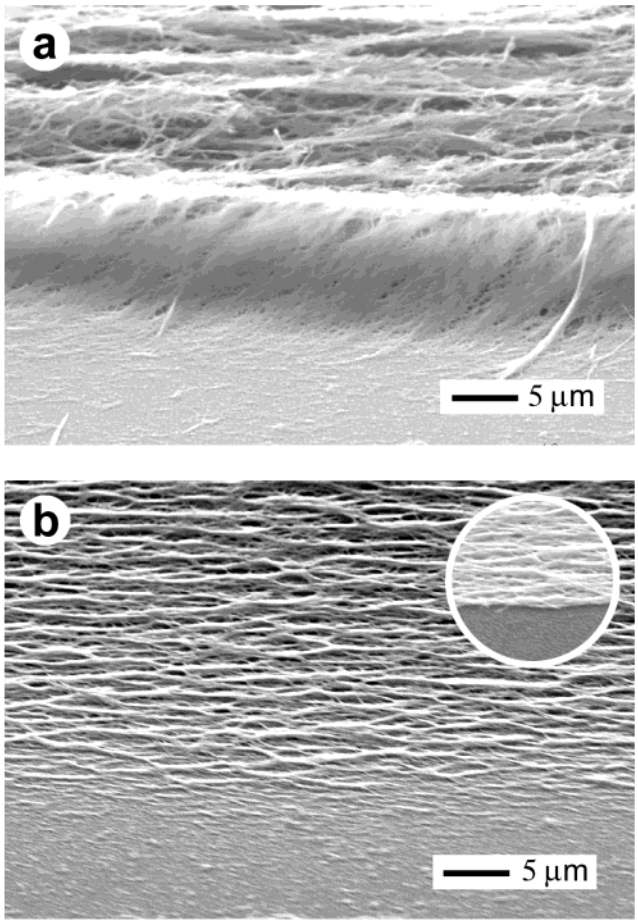

Figure 2. SEM micrographs of (a) bulk (using 365 nm unpolarized UV exposure) and (b) surface-localized (using 322 nm exposure) polymer networks templated on *homogeneously aligned* nematic BL006 host. The view shown is 45° to the substrate normal. The orientational order impressed on the network localized at the surface in part b is clearly maintained through the much bulk structure in part a, which is comparable to the 10 μm cell thickness. The inset shows the network in part b after scribing and reveals the true thickness of the surface layer.

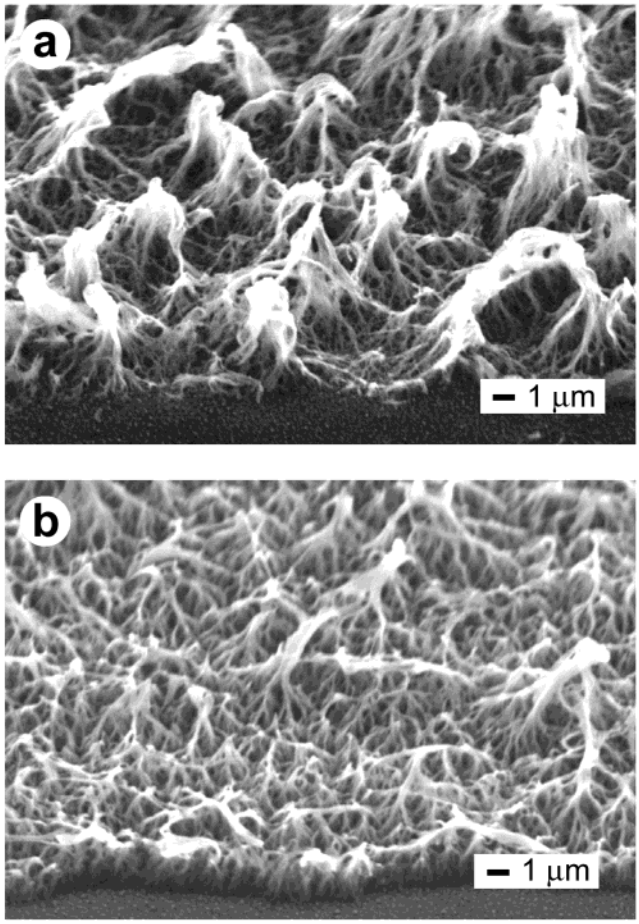

Figure 3. SEM micrographs of (a) bulk (using 365 nm unpolarized UV exposure) and (b) surface-localized (using 322 nm exposure) polymer networks templated on *homeotropically aligned* nematic BL006 host. The alignment was achieved by reorienting a homogeneously aligned optic axis by means of an electric field applied normal to the substrates. The view shown is 45° to the substrate normal. The structure in part a was observed on both substrates, indicating that the network extends through the full sample thickness. By contrast, the network in part b was completely localized on the substrate nearest the UV source.

applying an electric field (±50V, 1 kHz square wave) to rotate the LC molecules (director) to a vertical orientation. The consequent bulk network morphology (shown in Figure 3a after exposure to 365 nm UV) consists of fibrils and fibril bundles strongly oriented along the substrate normal, in sharp contrast to Figure 2. As in the example in Figure 2a, the network structure extends across the complete cell thickness (this was determined by estimating the length of partially collapsed bundles and accounting for the image tilt). Moreover, the structure in Figure 3a is found, essentially indistinguishably, on both substrates. In the surface-localized version (Figure 3b, 322 nm exposure), the polymer network is basically contained within a 2-μm thick layer on the incident substrate, but with a dominant vertical orientation. No significant evidence of network formation is observed on the "far" substrate. Because the same amount of monomer was used in preparing the two samples, there is higher areal density in the case of the surface-localized network (Figure 3b). In the bulk morphology (Figure 3a), thin fibrils are clumped together as they extend vertically away from the substrates and into the sample interior; the coarseness of this structure is presumably the result of a tradeoff between "vertical" growth (templated by the homeotropic orientation of the host liquid crystal) and the relatively low fraction of monomer. Finally, an interesting measure of the integrity of the homeotropic network structure on passing from the bulk to surface morphologies is that the liquid crystal host remains homeotropically aligned after the removal of applied field even in the case of the surface-localized network (Figure 3b). This is illustrated in Figure 4, which shows extinction of light passed perpendicularly through the sample, when it is placed between crossed polarizers and freely rotated about the substrate normal. By contrast, a region containing no network (i.e., masked from UV exposure) strongly transmits when the rubbing direction is rotated off the polarizer axes, indicating that the liquid crystal in the absence of a polymer network is homogeneously aligned by the substrate surface. Thus, the homeotropic surface network effectively reverses the strong planar anchoring conditions of the original, rubbed polyimide treatment of the substrate.

Depth control of an orientationally ordered polymer network is potentially quite useful in that it allows one to strike the appropriate balance between stabilization of a particular state of the host liquid crystal and minimization of the impact of the network on desirable

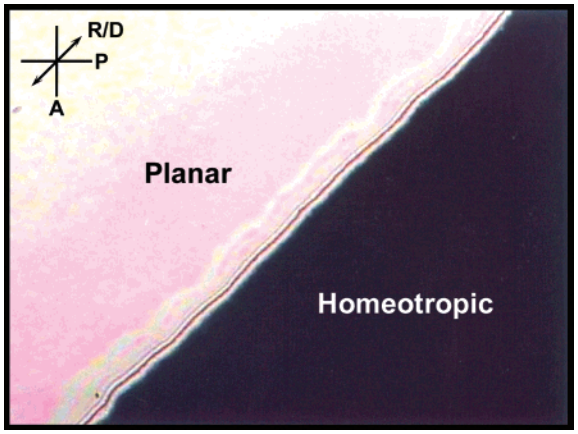

Figure 4. Optical micrograph of a homogeneously aligned nematic mixture masked from UV exposure (left, bright image) and the same mixture after reorientation to homeotropic state, formation of a surface network via 322 nm UV exposure, and subsequent removal of the electric field (right, dark image). The analyzer (A) is crossed with the polarizer (P) and is oriented at 45° to the direction of initial homogeneous alignment (R/D). The surface network clearly maintains the homeotropic state of the LC in the absence of the field and supersedes the effect of the original (homogeneous) alignment layer.

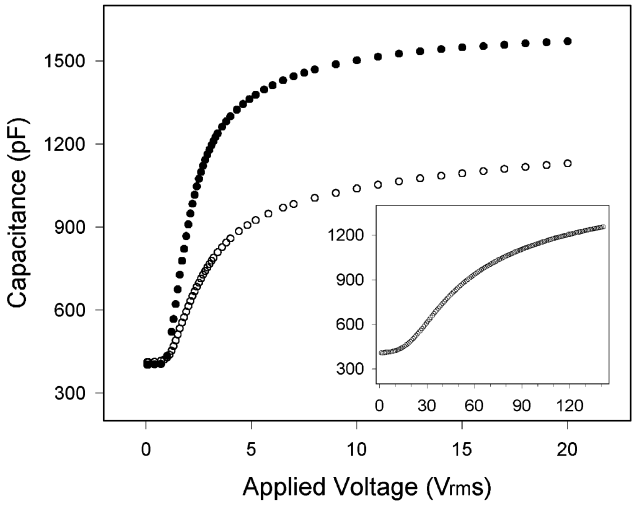

Figure 5. Measured capacitance (C) vs voltage applied to identical cells containing the LC mixture prior to polymerization (filled circles), after formation of a surface-localized polymer network (open circles), and after formation of a bulk polymer network (inset). In all cases, the increase in C corresponds to field-induced reorientation of the LC optic axis from an initially homogeneous to homeotropic orientation.

electrooptic properties of the liquid crystal. One crucial such property is response to low applied voltages. In Figure 5, we show the measured response of the capacitance C to applied voltage for three cells of fixed electrode area A and thickness d. One cell contains the unpolymerized initial mixture, and the other two contain the bulk or surface-localized polymer networks shown in Figure 2. In all cases, above a threshold voltage, C increases, and then begins to saturate. The threshold (∼1 V rms) and saturation (∼5 V rms) voltages are quite similar for the unpolymerized mixture and the sample containing the surface-localized network. The increase in $C = A\epsilon/d$ is due to director reorientation under the applied voltage, whereby the dielectric constant ϵ increases from $\epsilon_\perp$ to $\epsilon_\parallel > \epsilon_\perp$, with the subscripts referring to orientation of the electric field with respect to the director. However, for the sample with the bulk network (inset), both the threshold and saturation voltages for reorientation have increased by a factor ∼15. Thus, the surface network maintains the desired low voltage electrooptic effect of the host, while, as discussed above for the case of homeotropic orientation (Figure 3), still being fully capable of stabilizing a bulk distorted state of the liquid crystal. In contrast, the bulk network provides a large internal surface for anchoring the liquid crystal and consequently severely inhibits the response to applied voltages.

Conclusion

We demonstrated a simple method of controlling the formation of low concentration polymer networks in liquid crystal hosts along the "third" dimension—namely the direction normal to the substrates. By use of appropriate UV wavelengths and photopolymerization, networks with the same basic structural features and morphology driven by both kinetics- or diffusion-controlled polymerization and the host "template" may be distributed throughout the bulk or localized at a surface of the substrate. Using a simplified model of the network formation process, we determine that monomer diffusion dominates the development of the surface-localized networks in our system. While both surface and bulk polymer networks provide useful means of capturing basic structural features of liquid crystals in aligned or distorted states, the surface networks maintain important advantages, such as low operating voltage and minimal optical loss due to scattering, that are typically associated with low molecular weight liquid crystal-based devices.

Acknowledgment. This research was supported by the NSF/ALCOM under Grant No. DMR-8920147 and by the Office of Naval Research under Grant No. N00014-99-1-0899.

Supporting Information Available: Text giving the mathematical expressions for monomer diffusion during photopolymerization. This material is available free of charge via the Internet at http://pubs.acs.org.

References and Notes

(1) Doane, J. W. Polymer dispersed liquid crystals. In *Liquid crystals: Applications and Uses*; Bahadhur, B., Ed.; World Scientific: Singapore, 1990; Vol. 1, Chapter 14.
(2) Yang, D.-K.; Chien, L.-C.; Fung, Y. K. In *Liquid Crystals in Complex Geometries Formed by Polymer and Networks*; Crawford, G. P., Zumer, S., Eds.; Taylor & Francis: London, 1996; p 103.
(3) Hikmet, R. A. M. *J. Mater. Chem.* **1999**, *9*, 1921.
(4) Vorflusev, V.; Kumar, S. *Science* **1999**, *283*, 1903.
(5) Yamada, N.; Kohzaki, S.; Funada, F.; Awane, K. *SID Dig. Technol. Pap.* **1995**, 575.
(6) Sutherland, R. L.; Natarajan, L. V.; Tondiglia, V. P.; Bunning, T. J. *Chem. Mater.* **1993**, *5*, 1533.
(7) Sutherland, R. L.; Tondiglia, V. P.; Natarajan, L. V.; Bunning, T. J.; Adams, W. W. *Appl. Phys. Lett.* **1994**, *64*, 1074.
(8) Zhang, J.; Carlen, C. R.; Palmer, S.; Sponsler, M. B. *J. Am. Chem. Soc.* **1994**, *116*, 7055.
(9) Lee, S. N.; Sprunt, S.; Chien, L. C. *Appl. Phys. Lett.* **1998**, *72*, 885.
(10) Kang, S. W.; Sprunt, S.; Chien, L. C. *Appl. Phys. Lett.* **2001**, *78*, 3782.
(11) Nose, T.; Masuda, S.; Sato, S.; Li, J.; Chien, L. C.; Bos, P. J. *Opt. Lett.* **1997**, *22*, 35.
(12) Broer, D. J.; Heynderickx, I. *Macromolecules* **1990**, *23*, 2474.
(13) Heynderickx, I.; Broer, D. J. *J. Mater. Sci.* **1992**, *27*, 4107.
(14) Kang, S. W.; Sprunt, S.; Chien, L. C. *Appl. Phys. Lett.* **2000**, *76*, 3516.
(15) Kang, S. W.; Sprunt, S.; Chien, L. C. *Adv. Mater.* **2001**, *13*, 1179.

(16) Kang, S. W.; Sprunt, S.; Chien, L. C. *Polym. Prepr.* **2001**, *42* (2), 581.
(17) Noh, C. H.; Jung, J. Y.; Kim, J. Y.; Sakong, D. S.; Choi, K. S. *Mol. Cryst. Liq. Cryst.* **1993**, *237*, 299.
(18) (a) Rajaram, C. V.; Hudson, S. D.; Chien, L. C. *Chem. Mater.* **1995**, *7*, 2300. (b) Rajaram, C. V.; Hudson, S. D.; Chien, L. C. *Chem. Mater.* **1996**, *8*, 2460.
(19) Guiman, C. A.; Hoggan, E. N.; Clark, N. A.; Rieker, T. P.; Walba, D. M.; Bowman, C. N. *Science* **1997**, *275*, 57.
(20) Zhao, Y.; Chenard, Y. *Macromolecules* **2000**, *33*, 5891.
(21) van Nostrum, C. F.; Nolte, J. M.; Broer, D. J.; Fuhrman, T.; Wendorff, H. *Chem. Mater.* **1998**, *10*, 135.
(22) Broer, D. J.; Lub, J.; Mol, G. N. *Nature (London)* **1995**, *378*, 467.
(23) Hikmet, R. A. M.; Kemperman, H. *Nature (London)* **1998**, *392*, 476.
(24) Zhao, G.; Mouroulis, P. *J. Mod. Opt.* **1994**, *41*, 1929.
(25) Colvin, V. L.; Larson, R. G.; Harris, A. L.; Schilling, M. *J. Appl. Phys.* **1997**, *81*, 5913.
(26) (a) Broer, D. J.; Lub, J.; Van Nostrum, C. F.; Wienk, M. M. *Recent Res. Dev. Polym. Sci.* **1998**, *2* (Pt. 2), 313. (b) Broer, D. J.; Grietje, N. M.; van Haaren, J. A. M. M.; Lub, J. *Adv. Mater.* **1999**, *11*, 573.
(27) de Gennes, P. G.; Prost, J. *The Physics of Liquid Crystals*, 2nd ed.; Oxford University Press: Oxford, England, 1995; p 250.

MA020578O